Dr. Marios Maroudas

Working Group: J. M. Batllori, Y. Gu, D. Horns, M. Maroudas, J. Ulrichs

WISPFI: WISP Searches on a Fiber Interferometer

Motivation

- **Axions** solve the strong CP problem and are prominent candidates for CDM [1].
- Haloscope experiments are very sensitive in µeV but depend on the **local DM density** → poorly constrained → could be substantially smaller [2].
- LSTW experiments are not sensitive to QCD axions (conversion scales with $\mathbf{g}^4_{a\gamma\gamma}$).
- **High axion mass range** (meV to eV) is unexplored by direct detection experiments (except CAST [3]).
- Null results of direct DM searches → Need for **novel approaches**!

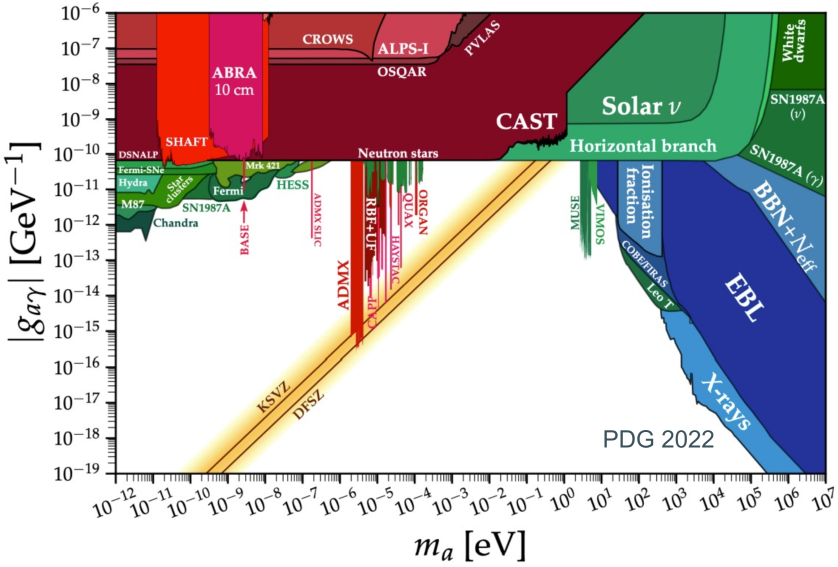

WISPFI (WISP searches on a Fiber Interferometer)

https://doi.org/10.48550/arXiv.2305.12969

- Novel table-top experiment focusing on **photon-axion conversion** in a waveguide by measuring **photon disappearance** in the presence of a strong external B field [4].
- Axion conversion probability scales with [5]:

  For $P_{\gamma\to a} \ll 1: \quad P_{\gamma\to a} \propto g_{a\gamma\gamma}^2 (BL)^2$

- Light guiding over **long distances** & **resonant detection** at a specially-confined region inside the bore of a strong magnet.
- **Mach-Zehnder interferometer** with the sensing arm inside the magnetic field.
- Expected signal: **amplitude reduction** & **phase shift.**

➢ No local DM density dependence.
➢ Operation at room temperature (no cryogenic setup required).

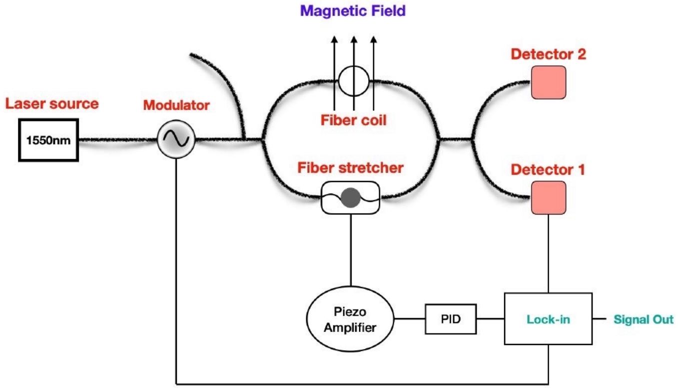

Photon-axion conversion

$$P_{\gamma\to a} = \underbrace{\sin^2(2\theta)}_{\text{Amplitude}}\underbrace{\sin^2(\pi L/L_{osc})}_{\text{Oscillations}}$$ [6]

Mixing angle: $\tan(2\theta) = 2\omega \frac{g_{a\gamma\gamma}B}{k_\gamma^2 - k_a^2}$

Photon, axion wave momenta

- Maximum conversion occurs for **large energy ω** or at **k_γ=k_a** (resonant conversion, θ = 45º).
- Axion mass at resonance in a medium with effective refractive index n_{eff}:

$$\boxed{m_a = \omega\sqrt{1 - n_{eff}^2}}$$

→ Required n_{eff} <1!

- For $P_{\gamma\to a} \ll 1$ the resulting probability becomes: $P_{\gamma\to a} \approx 10^{-18}\left(\frac{g_{a\gamma\gamma}}{10^{-12}\ GeV^{-1}}\right)^2\left(\frac{B}{10\ T}\right)^2\left(\frac{L}{200\ m}\right)^2$

Energy (ω) independent!

Hollow-Core Photonic Crystal Fibers (HC-PCF)

- Resonant conditions can not be fulfilled for wave-guides based on dielectric materials.
- HC-PCF guide light through a low-refractive index hollow core which is surrounded by a periodic arrangement of air-holes in the cladding this generating a photonic-bandgap structure [7].
- Through the bandgap structure, the propagating mode can acquire $\mathbf{n_{eff}<1}$ leading to real axion masses and resonant mixing.

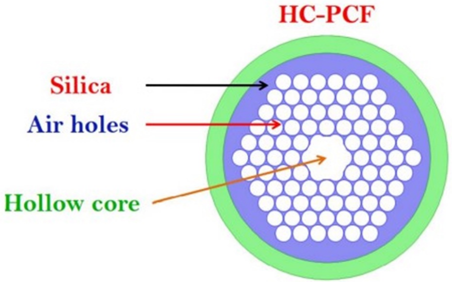

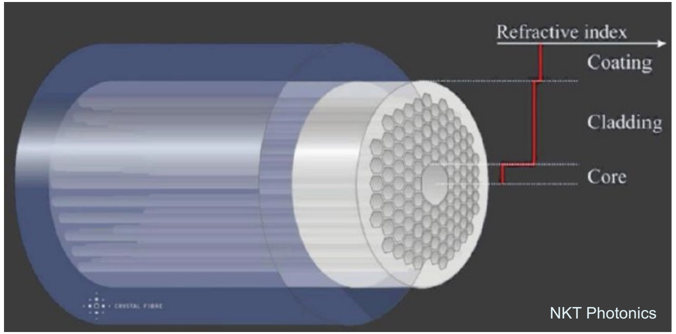

Effective mode index in HC-PCF (I)

- n_{eff} depends on the core radius (**R_c**), the bending radius (**R_b**), and the refractive index of the effective gas (n_{gas}) which in turn depends on pressure (**p**), wavelength (**λ**), and temperature (**T**) [8, 9].

- Analytical approximation [8]: $n_{eff} = \frac{k_\gamma}{k_o} = \sqrt{n_{gas}^2(\lambda, p, T) - \left(\frac{u_{nm}}{k_\gamma R_c}\right)^2}$

- FEM simulations studying the actual fiber geometry.

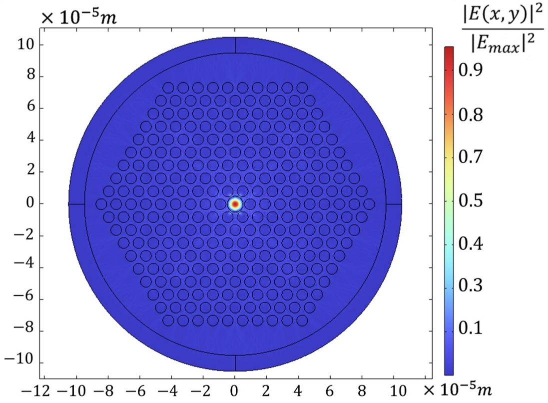

Mode field distribution of HC-PCF
($R_c = 5\mu m, p = 0.1bar, T = 20°C, n_{eff} = 0.992, n_{clad} = 1.45$)

Effective mode index in HC-PCF (II)

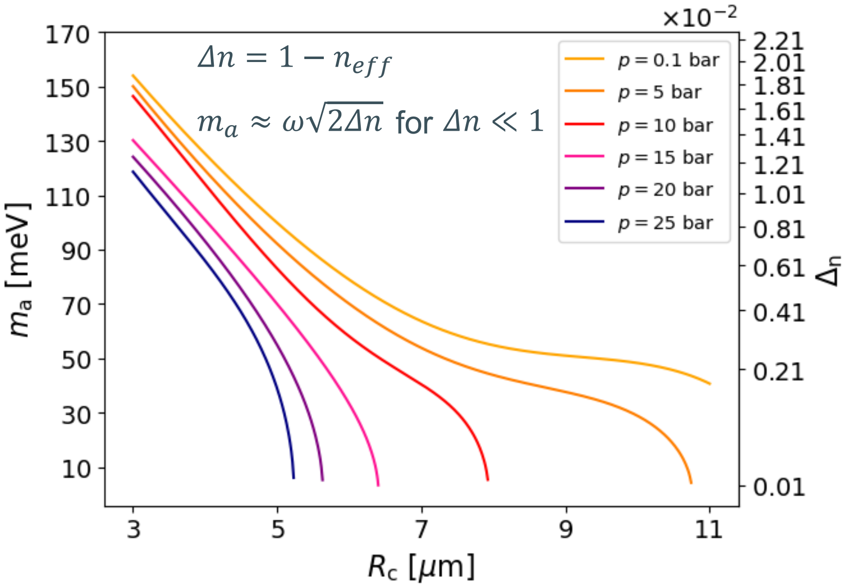

- Probed axion masses for resonant conversion based on different core radii (R_c) and pressures (p) of the air that fill the hollow core vary between **~ 10 meV** to **160 meV**.
- Observed increase of n_{eff} with increasing R_c and p matches the analytical approximation.

Effective mode index in HC-PCF (III)

- Wavelength of the propagating light and bending radius of the fiber also have an effect on the effective mode index.

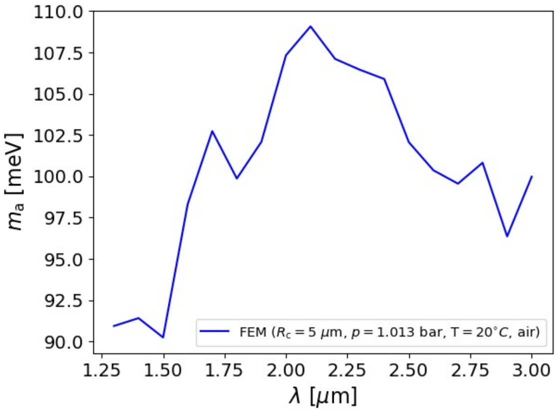

$$\Delta n = 1 - n_{eff} \qquad m_a \approx \omega\sqrt{2\Delta n}$$

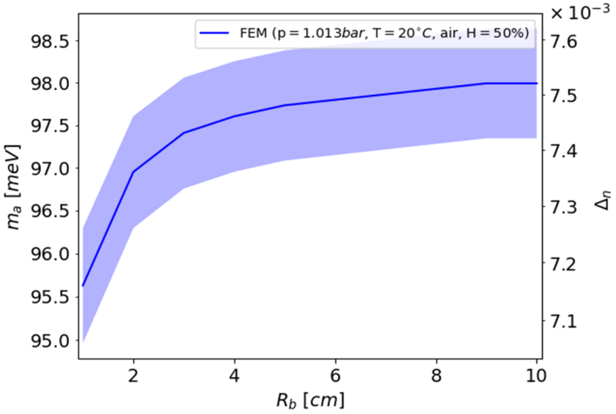

$$n'_{gas}(\lambda, p, T) = n_{gas}(\lambda, p, T) * n_{bend} = n_{gas}(\lambda, p, T) * \left(1 + \frac{R_c}{R_b}\right)$$

Experimental setup

- Partial free space partial fiber Mach-Zehnder-type interferometer.
- Sensing arm by HC-PCF placed in the magnetic bore and pressurized for tuning the probed axion mass.
- Both arms mounted on a voice coil (VC) for modulating the axion signal by shifting the position of the fiber coils and thus changing the effective B field.
- Fiber stretcher (FS) and temperature control pad (TCP) used for locking the interferometer via a PID.

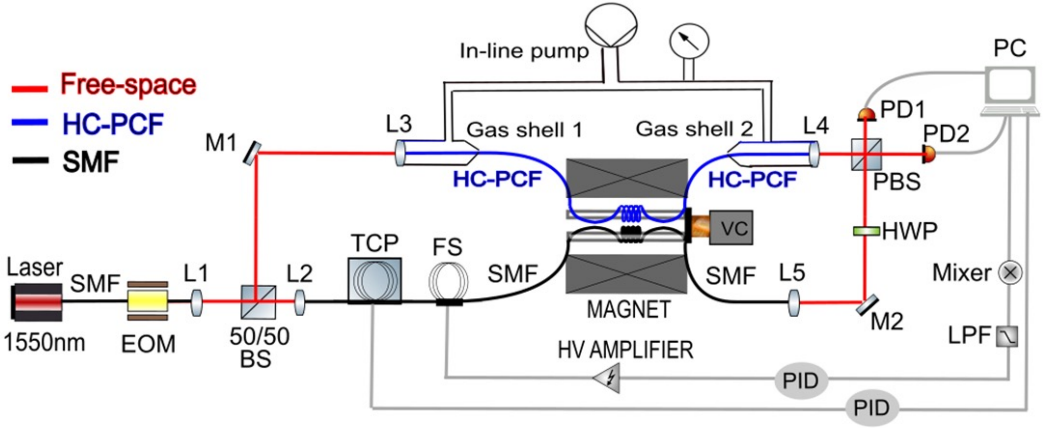

Sensitivity (I)

- MZI operated at dark fringe.
- Instrumental noise dominated by the dark current of the photo-detector.
- No additional losses.

$$g_{a\gamma\gamma} \approx 4\times10^{-13} GeV^{-1} \left(\frac{SNR}{3}\right)^{1/2} \left(\frac{B}{14T}\right)^{-1} \left(\frac{L}{500m}\right)^{-1} \left(\frac{P_{tot}}{4W}\right)^{-1/2} \left(\frac{\beta_{sig}}{1}\right)^{-1/2} \left(\frac{t}{180d}\right)^{-1/4} \left(\frac{NEP_{PD}}{0.5 fW/\sqrt{Hz}}\right)^{1/2}$$

- ➢ Axion mass mainly depends on core radius (R_c)
- ➢ HC-PCF production process leads to random variations of the R_c which widen the probed axion mass range but reduce the sensitivity.

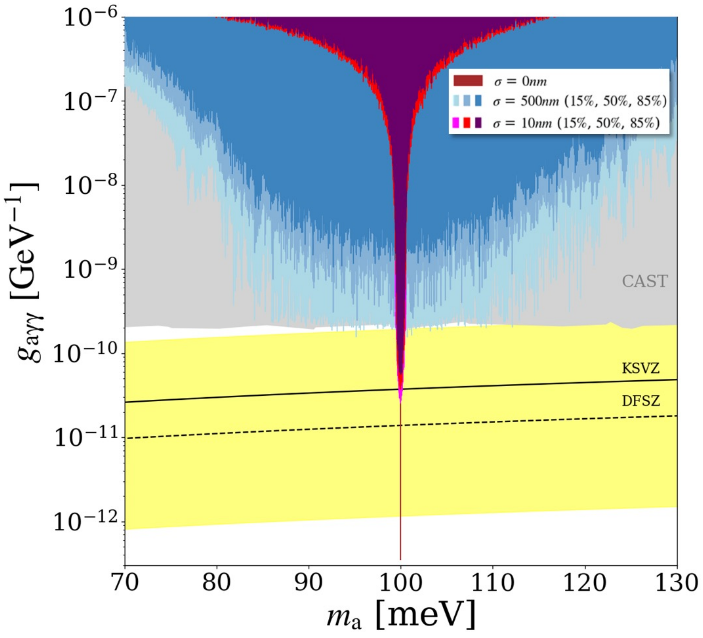

Sensitivity (II)

A. Baseline setup: 4 W laser @ 1550 nm,
B = 14 T, 500 m HC-PCF at standard conditions.

B. Long term projection: 40 W laser @ 1550 nm,
B = 14 T, 1 km PM HC-PCF with σ=10 nm.

- Tuning from 0.1 – 23 bar in 116 steps of 0.6 meV between 50 – 100 meV

→ **DFSZ sensitivity in a wide axion mass range!**

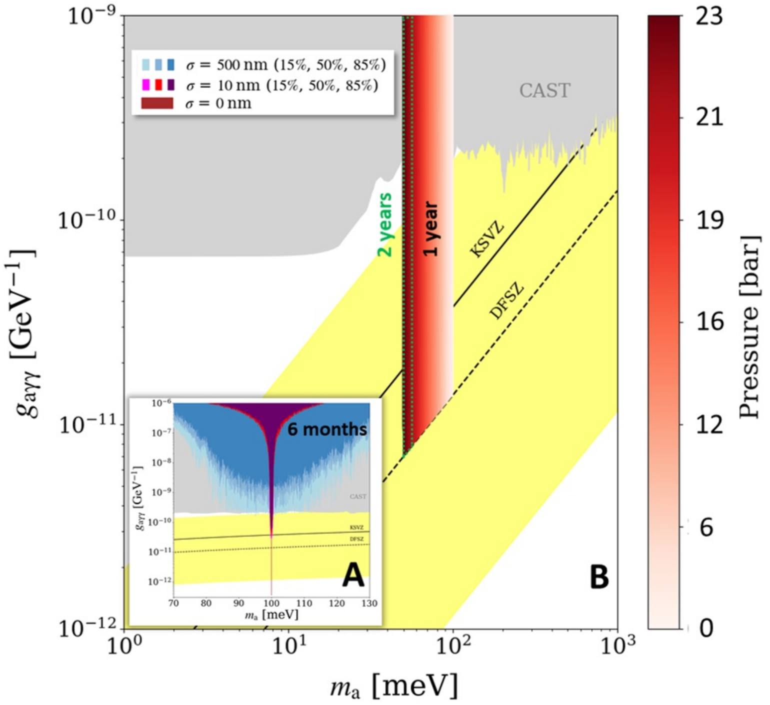

Future steps

- Test HC-PCF fiber in the 14 T warm-bore solenoid magnet.
- Signal modulation with VC / wavelength modulation.
- Interferometer locking in amplitude/phase and temperature for larger fiber lengths (~100m).
- Integration to free-space (ongoing).
- Noise optimization.
- Final commissioning and data acquisition.
- Electric field conversion experiment (WISPFI-E) using coaxial capacitor.

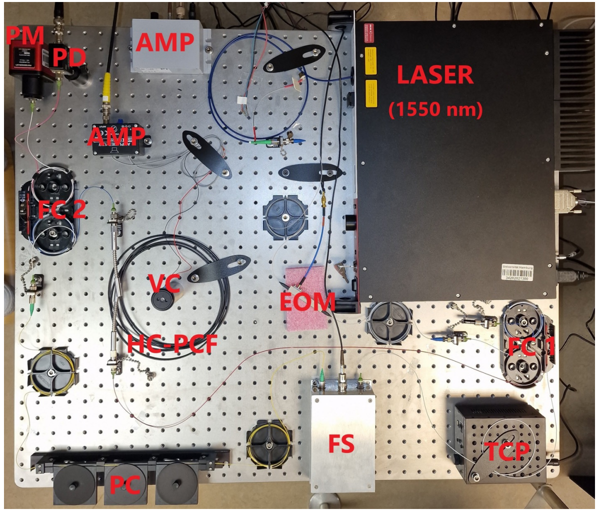

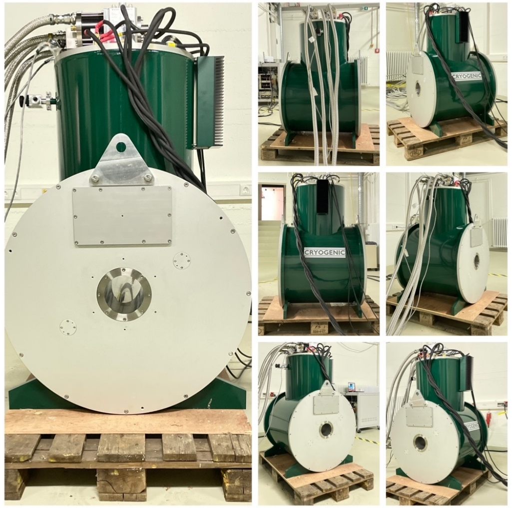

Summary

- Light guiding through **waveguide** embedded in a strong B field.
- Partial free-space, partial fiber **Mach-Zehnder**-type interferometer.
- **Amplitude/phase reduction/shift** in the presence of γ→a conversion.
- **HC-PCF** meets the conditions for resonant mixing.
- **Tuning** in a wide axion mass range by regulating the **gas pressure** in the fiber.

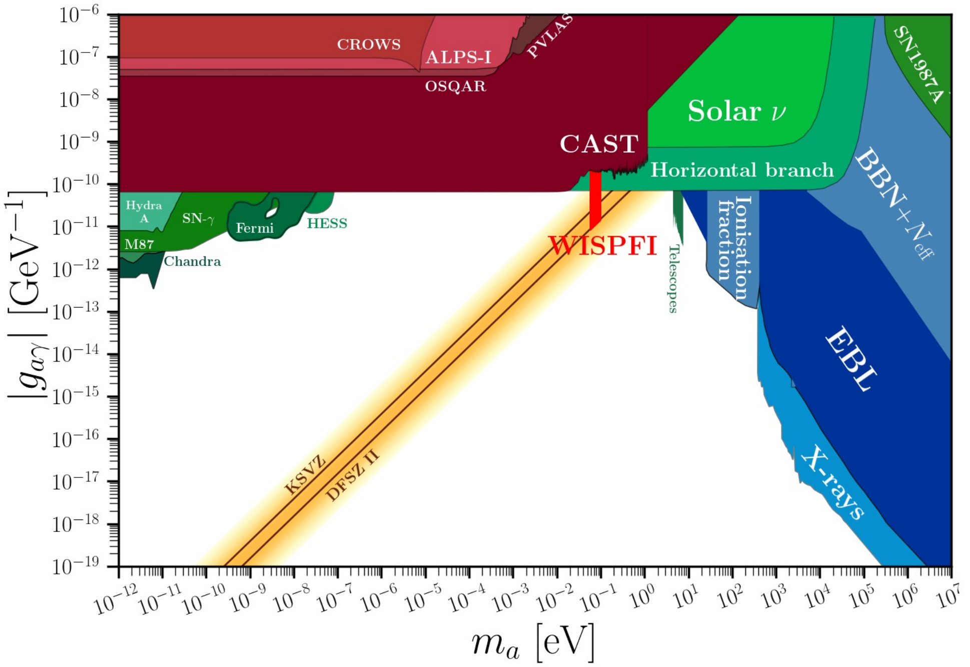

https://doi.org/10.48550/arXiv.2305.12969

Universität Hamburg
DER FORSCHUNG | DER LEHRE | DER BILDUNG

CLUSTER OF EXCELLENCE
QUANTUM UNIVERSE

Thanks for your attention!

Find out more about the cluster:
www.qu.uni-hamburg.de

References

(1) R. D. Peccei, H. R. Quinn, CP Conservation in the Presence of Pseudoparticles, Phys. Rev. Lett. 38, 1440 (**1977**), https://doi.org/10.1103/PhysRevLett.38.1440
(2) B. Eggemeier et al., Axion minivoids and implications for direct detection, Phys. Rev. D 107, 083510 (**2023**), https://doi.org/10.1103/PhysRevD.107.083510
(3) V. Anastssopoulos et al., New CAST limit on the axion-photon interaction, Nature Phys.13, 584-590 (**2017**), https://doi.org/10.1038/nphys4109
(4) J. M. Batllori, et al, WISP Searches on a Fiber Interferometer under a Strong Magnetic Field, arXiv (**2023**), https://doi.org/10.48550/arXiv.2305.12969
(5) H. Tam, Q. Yang, Production and detection of axion-like particles by interferometry, Phys. Lett. B, 716, 435-440 (**2012**), https://doi.org/10.1016/j.physletb.2012.08.050
(6) G. Raffelt, L. Stodolsky, Mixing of the photon with low-mass particles, Phys. Rev. D 37, 1237 (**1988**), https://doi.org/10.1103/PhysRevD.37.1237
(7) P. Russell, Photonic Crystal Fibers, Science 299, 5605 (**2003**), https://doi.org/10.1126/science.1079280
(8) E. A. J. Marcatili, R. A. Schmeltzer, Hollow Metallic and Dielectric Waveguides for Long Distance Optical Transmission and Lasers, Bell System Technical Journal 43, 4, (**1964**), https://doi.org/10.1002/j.1538-7305.1964.tb04108.x
(9) L. Rosa et al., Analytical Formulas for Dispersion and Effective Area in Hollow-Core Tube Lattice Fibers, Fibers 9, 10, (**2021**), https://doi.org/10.3390/fib9100058

Backup Slides

Effective mode index in HC-PCF

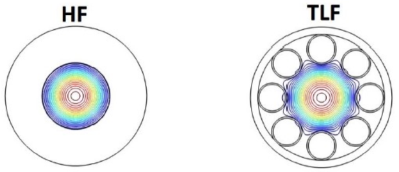

$$n_{eff} = \frac{k_\gamma}{k_o} = \sqrt{n_{gas}^2(\lambda, p, T) - \left(\frac{u_{nm}}{k_\gamma R_c}\right)^2}$$

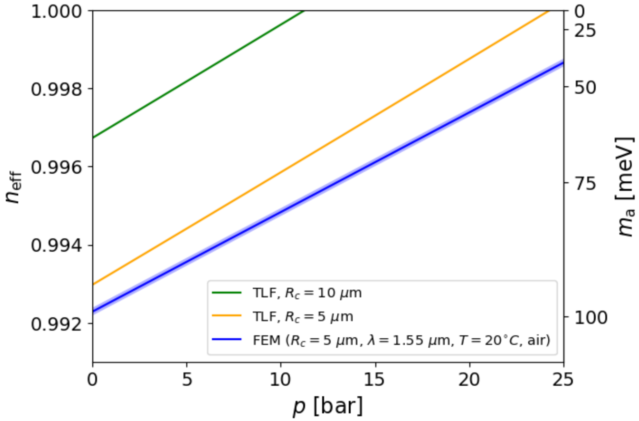

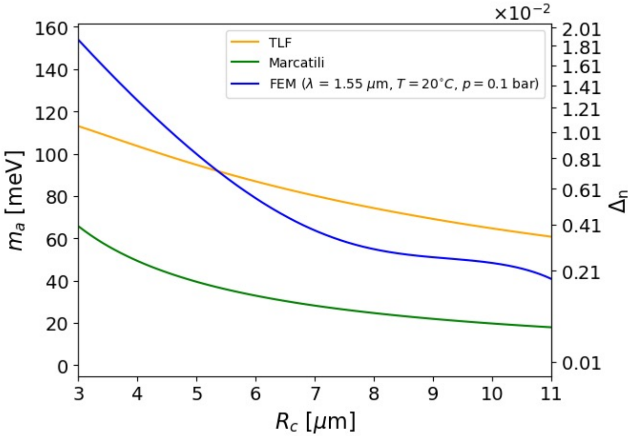

Confinement losses

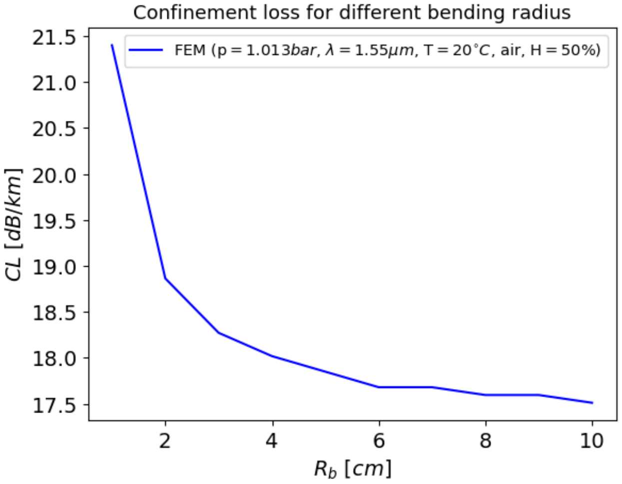

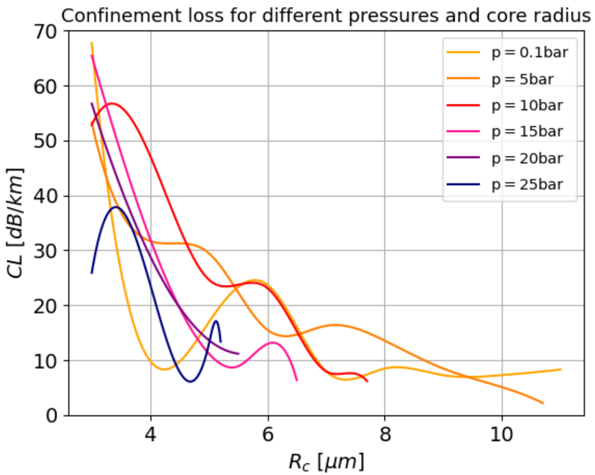

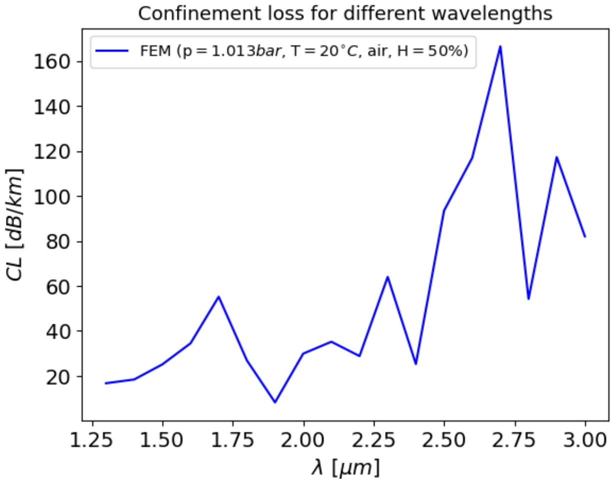

$$CL[dB/km] = -\frac{20}{\ln 10} \cdot \frac{2\pi}{\lambda} \cdot \mathrm{Im}(n_{eff})$$

Refractive index of air

- Refractive index of air as a function of pressure and temperature for T=20^{o}C and P=1.013 bar accordingly.